Voxel-level analysis of normalized DSC-PWI time-intensity curves: a potential generalizable approach and its proof of concept in discriminating glioblastoma and metastasis.

AUTHORS AND AFFILIATIONS

Albert **Pons-Escoda**[1,2],
Alonso **Garcia-Ruiz**[3]
Pablo **Naval-Baudin**[1]
Francesco **Grussu**[3],
Juan Jose **Sanchez Fernandez**[1]
Angels **Camins Simo**[1]
Noemi **Vidal Sarro**[4,2]
Alejandro **Fernandez-Coello**[5,6,7]
Jordi **Bruna**[2]
Monica **Cos**[1]
Raquel **Perez-Lopez**[3,8]
Carles **Majos**[1,2,]

Albert Pons-Escoda and Alonso Garcia-Ruiz share first joint authorship.

1. Radiology Department, Institut de Diagnòstic per la Imatge- IDI, Hospital Universitari de Bellvitge.
2. Neurooncology Unit, Institut d'Investigació Biomèdica de Bellvitge- IDIBELL.
3. Radiomics Groups, Vall d'Hebron Institut d'Oncologia.
4. Pathology Department, Hospital Universitari de Bellvitge.
5. Neurosurgery Department, Hospital Universitari de Bellvitge.
6. Pathology and Experimental Therapeutics Department, Anatomy Unit, University of Barcelona.
7. *Biomedical Research Networking Centers* of Bioengineering, Biomaterials and Nanomedicine (CIBER-BBN).
8. Radiology Department, Hospital Universitari Vall d'Hebron.

Voxel-level analysis of normalized DSC-PWI time-intensity curves: a potential generalizable approach and its proof of concept in discriminating glioblastoma and metastasis

ABSTRACT

OBJECTIVE

Standard DSC-PWI analyses are based on concrete parameters and values, but an approach that contemplates all-points in the time-intensity-curves and all-voxels in the region-of-interest may provide improved information, and more generalizable models. Therefore, a method of DSC-PWI analysis by means of normalized time-intensity-curves point-by-point and voxel-by-voxel is constructed, and its feasibility and performance are tested in presurgical discrimination of glioblastoma and metastasis.

METHODS

In this retrospective study, patients with histologically confirmed glioblastoma or solitary-brain-metastases and presurgical-MR with DSC-PWI (August2007–March2020) were retrieved. The enhancing-tumor and immediate-peritumoral-region were segmented on CE-T1wi and coregistered to DSC-PWI. Time-intensity-curves of the segmentations were normalized to normal-appearing-white-matter. For each participant, average and all-voxel-matrix of normalized-curves were obtained. The 10 best discriminatory time-points between each type of tumor were selected. Then, an intensity histogram analysis on each of these 10 time-points allowed the selection of the best discriminatory voxel-percentile for each. Separate classifier models were trained for enhancing-tumor and peritumoral-region using binary logistic regressions.

RESULTS

A total of 428 patients (321glioblastomas, 107metastases) fulfilled the inclusion criteria (256men; mean-age, 60years; range, 20-86years). Satisfactory results were obtained to segregate glioblastoma and metastases in training and test sets with AUCs 0.71-0.83, independent accuracies 65%-79%, and combined accuracies up to 81%-88%.

CONCLUSION

This proof-of-concept study presents a different perspective on brain MR DSC-PWI evaluation by the inclusion of all-time-point of the curves and all-voxels of segmentations to generate robust diagnostic models of special interest in heterogeneous diseases and populations. The method allows satisfactory presurgical segregation of glioblastoma and metastases.

KEYWORDS

- Brain Neoplasms
- Glioblastoma
- Metastases
- Magnetic resonance imaging
- Perfusion imaging

KEY POINTS

- An original approach to brain MR DSC-PWI analysis, based on a point-by-point and voxel-by-voxel analysis of normalized time-intensity curves is presented.
- The method intends to extract optimized information from MR DSC-PWI sequences by impeding the potential loss of information that may represent the standard evaluation of single concrete perfusion parameters (cerebral blood volume, percentage of signal recovery, or peak height) and values (mean, maximum or minimum).
- The presented approach may be of special interest in technically heterogeneous samples, and intrinsically heterogeneous diseases. Its application enables satisfactory presurgical differentiation of GB and metastases, a usual but difficult diagnostic challenge for neuroradiologist with vital implications in patient management.

ABBREVIATIONS

CBV cerebral blood volume

ET enhancing tumor

NAWM normal-appearing white matter

nTIC normalized time-intensity curve

PH peak height

PR peritumoral region

PSR percentage of signal recovery

TIC time-intensity curve

INTRODUCTION

Presurgical diagnosis of brain tumors is of vital importance for patient management. While histopathology remains the final reference standard, the presurgical approach mainly lays on neuroimaging with Magnetic Resonance (MR) as the lead actor. In this sense, one of the most challenging differentials for neuroradiologists is glioblastoma (GB) versus solitary brain metastasis, the two most common malignant intracranial tumors in adults[1, 2]. It is a cause of frequent debate in neurooncology units, whether the patient has a known extracranial primary tumor or not. The ability to presurgically differentiate these two entities will significantly impact further steps on therapeutic decisions[3–8]. Consequently, achieving the highest diagnostic accuracy with non-invasive assays is an unmet critical need in the clinical practice.

Unfortunately, both tumor types are highly heterogeneous in their presentations, and morphological MR is too often limited to reach a trustable diagnosis[9, 10]. For this reason, the use of so-called “advanced” or “functional” MR-imaging techniques in this context has been growing in recent years. These techniques go beyond morphology to offer information on the metabolic, cellular, or vascular environment levels. One of these MR techniques is Dynamic Susceptibility Contrast- Perfusion Weighted Imaging (DSC-PWI), which has shown promising results for the diagnosis of brain tumors[11–13].

DSC-PWI has been correlated with different histological features of tumor vascularization, microvascularity and blood-brain-barrier integrity[14–20]. In this respect, prior work has shown that tumor vasculature significantly differs between glioblastoma and metastasis. GB is characterized by heterogeneous blood-brain-barrier disruption, while in metastasis, blood-brain-barrier is absent and angiogenesis is the predominant phenomenon. Regarding the peritumoral-region, metastases cause pure vasogenic edema, while in GB, infiltrative tumor cells may be found among edema[11, 21–24]. DSC-PWI exploits these tissular characteristics to try to monitor and discriminate different tumor types and environments.

Many authors have tried to presurgically differentiate GB and metastasis based on DSC-PWI[25, 26, 35–41, 27–34]. Among the different studies, many different perfusion parameters are used, with a high heterogeneity in the results and thresholds. The most evaluated classical parameters are cerebral blood volume (CBV), percentage of signal recovery (PSR), and peak height (PH). These are all extracted from DSC-PWI time-intensity curves (TICs). Prior work has suggested that analyzing and comparing the entire TIC instead of these concrete parameters may provide better information, by means of normalized TICs (nTICs) that can be compared individually or combined to train predictive models[42].

Furthermore, the standard parameters are usually evaluated in terms of mean or extreme (minimum or maximum) values obtained from the voxels in the region of interest (ROI). We consider this kind of approach further discards potentially useful information by not accounting for atypical distributions of these parameters. This atypical spatial distribution of perfusion may be, actually, common in some cases of predominant heterogeneity, as the current scenario of GB and metastases, which are proved highly heterogeneous tumors on histology[21–24].

We hypothesize that the study of the entire nTIC and the whole range of voxels included in the volumetric segmentations of enhancing tumor and peri-enhancing region could provide more accurate tissue characterization and improve tumor classification. Furthermore, the use of normalized perfusion data and model training based on all-

timepoints and all-voxels offers a new perspective in MR-perfusion imaging which should facilitate the construction of more robust and generalizable models than isolated parameters such as CBV, PSR or PH, by being able to take into account tumoral and technical heterogeneity more completely.

With these considerations in mind, we aim to present this novel method of DSC-PWI nTICs percentile histogram voxel-level analysis and test it for the clinical discrimination of glioblastoma and metastasis.

MATERIAL AND METHODS

This work was approved by the Research Ethics Committee of Hospital Universitari de Bellvitge. A waiver of a specific informed consent was provided by the ethics committee for this retrospective study.

Patients

Newly diagnosed patients with histologically confirmed GB or solitary brain metastases (August 2007–March 2020) were retrospectively retrieved from our center's database. Inclusion criteria for the study were as follows: 1) confirmed tumor diagnosis by histology according to The World Health Organization 2007 or 2016 criteria[43, 44], 2) an available diagnostic presurgical MR imaging examination including DSC-PWI and contrast-enhanced T1WI (CE-T1WI), 3) enhancing tumor on CE-T1WI with the shortest diameter of at least 10 mm.

Imaging

All the MR imaging examinations included in the study were acquired in the same hospital with 1 of 3 different scanners: Ingenia 3T with a 32-channel head coil, Ingenia 1.5T, or Intera 1.5T both with a 16-channel head coil (Philips Healthcare). Acquisition parameters for DSC-PWI (all gradient echo) and CE-T1WI sequences are summarized in Supplemental Table1, and DSC-PWI technique distribution between groups is specified in Supplemental Table2. The intravenous contrast (gadobutrol; 1 mmol/mL, 0.1 mmol/kg) injection protocol was as follows: 18- or 20-ga peripheral intravenous access. No preload was performed. Baseline acquisition was on the order of 10 points. The automatic injection start (power injector at 4–5 mL/s) was by a manual setting. A final bolus of saline (25–50 mL) was injected at the same speed. The time and number of dynamics ranged from 1.26 to 3.55 seconds and 30 to 60, respectively. The quality of the sequences was evaluated by visual inspection by 2 neuroradiologists (A.P.-E. and C.M.) with more than 6 and 25 years of experience in MR imaging of brain tumors. The examinations were labeled as poor quality and excluded from the study under the following circumstances: 1) artifacts prevented enhancing tumor segmentation on CE-T1WI or coregistration of CE-T1WI and DSC-PWI, or 2) an obvious low signal-to-noise ratio was observed in the raw TICs.

Postprocessing

The enhancing tumor (ET) and contralateral normal-appearing-white-matter (NAWM) were segmented on CE-T1WI using a supervised semiautomatic volumetric method with histogram thresholding and morphologic operations. The peritumoral region (PR) segmentation included a 2 cm wide rim of brain parenchyma immediately around the ET, excluding ventricles and extraaxial spaces and structures. Segmentations were then

coregistered with DSC-PWI. Necrosis was excluded from the segmentations as it is avascular tissue which does not generate time-intensity curves. A 2 cm rim of PR was used because this is the distance around the enhancing tumor where it is assumed that most brain microinfiltration occurs in GB, and which is consequently used for concomitant radiotherapy planning as the "safety-margin" to be treated[45–48]. We used semiautomatic volumetric segmentations instead of partial, manual, or single-section ROI selection methods in order to minimize operator-dependency as well as to include all the intrinsic heterogeneity of the tumors in the analysis. 3D Slicer, Version 4.10 (http://www.slicer.org) was used for segmentation, and the BRAINSFit module of 3D Slicer, for coregistering.

All TICs included for analysis were normalized following the method proposed by Pons-Escoda et al [42], generating multiple normalized TICs (nTICs). For each participant, we obtained the following nTICs: average curve of all ET voxels, average curve of all PR voxels, a matrix of nTICs for all segmented voxels in the ET, and another matrix in the PR. The matrices had as many nTICs as voxels included in the segmentations. All resultant nTICs are superimposable and comparable between patients in a single graph, as they are composed of the same number of time-matching points and intensity units normalized to NAWM.

The TICs were processed using Python 3.6 software (https://www.python.org/downloads/release/python-360/).

Data Analysis

The study sample was split into "training" (70%) and "test" (30%) subsets. The groups were balanced by date of examination to minimize the impact of quality and technical differences between TICs of the more distant-in-time exams.

The 10 best discriminatory time-points were selected by performing area under the curve-receiver operating characteristic (AUC-ROC): the analysis was performed for all time-points on the segmentation-average ET and PR nTICs of the training subset, and those 10 points with the highest AUC were the chosen. Ten was selected semi-arbitrarily as the highest number of information to be included with acceptable AUC-ROCs and while avoiding overtraining[49, 50].

Then, an intensity histogram analysis was performed on each of these 10 time-points to select the voxel percentile which showed greater differences between groups. This produced 10 histograms for ET segmentation and 10 for the PR segmentation (1 histogram for each discriminatory time-point). These histograms depict the signal-intensity distribution of all the voxels included in the segmentations for each discriminatory time-point. For each time-point, the voxel percentile that showed greater differences between tumor-types was selected.

Subsequently, separate classifier models were trained for the ET and PR segmentations using binary logistic regression on these 10 variables on the "training" subset. The best discriminatory thresholds of the algorithms were obtained by receiver operating characteristic (ROC) analysis. Finally, the constructed classifiers and thresholds were applied to the "test" set.

Additionally, we also analyzed the classification performance of average nTICs, in order to compare the present method with a previous method that compared average nTICs, without performing the voxel- level percentile histogram-intensity analysis[42].

All the statistical computations were performed with R statistical and computing software, Version 3.5.1 (http://www.rproject.org).

RESULTS

Patients

A total of 428 patients (321 glioblastomas and 107 metastases) fulfilled the inclusion criteria (256 men; mean age, 60 years; range, 20-86 years). A partial overlap of 48 glioblastomas and 49 metastases which participated in a prior published study with different objectives and methodology[42] is reported. The flow diagram of study participants is shown in Figure1. Demographics of the study sample are summarized in Table1. Three GBs and 3 metastases were ruled out by the quality filter. As a result, 318 GB and 104 metastases were included in the final dataset (total n=422). The Metastases dataset was split into training (70%) and test (30%) subsets. The same resultant number of GB were included in the training set, and the remaining number was left for testing. Our intention with this was to avoid overweighting of the classifier to the most prevalent tumor type (glioblastoma) in our set. The resultant subsets were as follows: training, 73 GB and 73 metastases; test, 245 GB, and 31 metastases. The lesser proportion of metastases is justified by the fact that only single or grouped oligometastases, which hypothetically created real diagnostic doubts on daily practice, were included in the study.

nTIC and Percentile Histogram Analysis

Average ET and PR nTICs for each tumor type and the 10 discriminatory time-points are shown in Figure2. Notable differences were found between each tumor type nTICs on a first visual assessment. The most obvious were around the maximal signal intensity drop and the signal recovery segments.

The classifier algorithms are shown in Figure2 with the 10 best discriminatory points, the selected intensity-percentiles, and the model coefficients for each.

Satisfactory results were obtained to segregate GB and metastases with the constructed classifiers. In the training set (ET AUC = 0.81, accuracy = 79%; PR AUC = 0.83, accuracy = 78%). In the test set (ET AUC = 0.79, accuracy = 71%; PR AUC = 0.71, accuracy = 65%). Moreover, improved results were obtained when combining matching classifications of the ET and PR (72% of classifications matched in training set providing 88% accuracy. In the test set, 61% of classifications matched, providing 81% accuracy). Results are summarized in Table2 and Figure3.

Additionally, the performance of whole segmented ROIs average nTICs was poorer in training and test sets for both the ET (training accuracy = 71%; test accuracy = 70%) and PR (training accuracy = 73%; test accuracy = 61%).

Figure4 depicts an example of the classifier applicability.

DISCUSSION

In this study, we applied the previously reported nTIC methodology[42] to retrospectively analyze DSC-PWI studies of glioblastomas and metastasis, and explored its applicability for the discrimination between these two tumor-types. We adapted the method to better approach the tumors' inherent high histological, vascular, and microvascular heterogeneity. The new modified method allows constructing classifiers that take into account the lesions' heterogeneity on a voxel-level by performing a point-by-point percentile histogram analysis of nTICs to generate a classifier model based on optimal

time-points and optimal voxels. We obtained satisfactory results that provided up to 81% accuracy discrimination between glioblastoma and metastasis in the test set.

Reliable presurgical differentiation of GB and metastasis is crucial as management of these two entities differs significantly. While a suspected GB should undergo maximal safe gross surgical resection as treatment of choice, suspected metastases require systemic staging or re-staging before determining different local therapeutic approaches combined with systemic treatments[3, 4]. For example, if a metastasis were to be surgically removed under the erroneous assumption of glioblastoma, the overall benefit of this potential morbid approach is lost or unknown [5, 6]. Moreover, improving the accuracy of the radiological assessment may be also relevant in patients with radiologically suspected GB, who are not candidates for specific therapeutic procedures due to their performance status or high basal morbidity, and in whom the final diagnostic assumption rests solely on neuroimaging[7]. This also applies in a vast majority of patients with known systemic primary tumor and brain lesion suspicious of brain metastasis, who are directly treated for an assumed brain metastasis without confirmative histology[4], despite the knowledge that some of these tumors may end up not corresponding to the assumed histology[8]. These different scenarios in which the MR imaging diagnosis is the key to patient management warrant the highest possible diagnostic accuracy.

DSC-PWI is an MR imaging technique that can currently be performed on most MR imaging units and which provides a noninvasive in vivo assessment of microvascular systems. It consists of a dynamic temporal acquisition during the vascular first pass of a contrast bolus. The injection of gadolinium results in an initial reduction in T2 signal intensity of the tissue, followed by signal recovery during contrast washout. The TICs can be extracted from this process. Well-studied parameters such as CBV, PSR or PH are generated from these curves. The CBV corresponds to the area under the curve and is usually measured relative to the NAWM (relative CBV). It has been correlated to histologic measurements of tumor vascularization[14, 20, 38]. The PSR and the PH are measured relative to the TIC baseline. PSR may quantify the predominant T1 effect (signal recovery above baseline) or T2 effect (signal recovery below baseline). These effects represent different leakage phenomena, which are explained by a complex combination of blood-brain barrier permeability, vascular volume fraction and vessel size, and tumor cell size and density[14, 17, 38]. The more recently popularized parameter PH is a measure with hypothetical parallelism to rCBV and also potentially related to tumor vascularization[29, 31]. Tumor vascularity is known to be different between GB and metastasis, and these differences could be monitored with DSC-PWI. Both tumors are heterogeneous, but their classical hallmarks are heterogeneous blood-brain-barrier disruption in GB and angiogenesis in metastases. Regarding the peritumoral-region, metastasis cause pure vasogenic edema, while GB associates infiltrative tumor cells among the perilesional edema[11, 21–24]. These histological features seem to be represented in the case of GB mainly by a higher PSR in the enhancing-tumor[25, 26, 30, 31] and a higher CBV in the peritumoral-region[25, 27, 37, 28–30, 32–36]. Some authors also report higher CBV in the enhancing-tumor[26], or higher PSR[31] and PH[29, 31] in peritumoral-region. On the other hand, some papers are unable to find significant differences between GB and metastasis with any of these variables[38–41]. As previously stated, analyzing the entire TIC instead of these concrete parameters, may provide improved information[42]. On the other hand, the heterogeneous results in the different papers evaluating DSC-PWI could be at least partially explained by technical variability between studies. The nTICs method allows

performing unsupervised point-by-point curve analysis to minimize the influence of technical parameters on the results.

DSC-PWI pulse-sequence parameters (Flip Angle and Time of Echo), influence curve morphology and thus affect the value of CBV and PSR, often paradoxically[16–18]. For this reason, the best results in the literature are obtained from homogeneous populations, but the best discriminatory parameters and thresholds vary between these studies. Meanwhile, those papers that do include technical heterogeneities, do not achieve optimal results. At this respect, our center's sample has changing DSC-PWI parameters between MRI scanners and between years, and may be a paradigm of heterogeneity, which is probably also the real-life scenario for most clinical centers worldwide. Indeed, this is why it is important to develop a method which can minimize the impact of technical variability on perfusion metrics. We hypothesize that in heterogeneous samples with non-standardized technical acquisition characteristics, the evaluation of the whole nTIC would be more powerful than standard approaches, as the paradoxical effects of pulse-sequence parameters would be better integrated.

Moreover, it is well known that GB and metastases are histologically highly heterogeneous tumors[21–24], so an approach which takes into account this heterogeneity by selecting the best predictive habitats seems necessary to obtain the best performing results. Most works in this field contemplate only mean, maximum or minimum values for each evaluated parameter (CBV, PSR, PH). This kind of approach disregards most of the values contained within the whole tumor, even though the best discriminating value might not be one of these isolated metrics.

For all these reasons, we propose an approach for analyzing nTICs based on a volumetric voxel-by-voxel histogram evaluation of the enhancing-tumor and the immediate peritumoral-region with semi-unsupervised selection of the discriminatory time points and voxel percentile. With this approach we aim to face the issue of tumors' vascular heterogeneity and maximize the discriminatory capacity of DSC-PWI. In summary, our approach not only minimizes the impact of physiological and technical variability, but also avoids the problem of choosing a concrete DSC-PWI parameter to analyze. We achieve these goals by selecting the most discriminatory time-points in the nTICs and then selecting the most discriminatory voxel-intensity percentile for those time-points.

Another potential weakness in DSC-PWI literature is the inhomogeneity in ROIs selection method. Many of these studies do not include the whole tumor, while others are operator dependent, focusing on extreme values such as "hot-spots" or tumor average. We minimized operator-dependent variability by performing volumetric segmentations of the whole enhancing tumor and statistical unsupervised selection of discriminatory variables without prior knowledge inputs.

Some limitations of our paper must be considered. The single-site and retrospective character of the analysis may affect reproducibility, so multicentric and prospective studies in new real clinical scenarios are needed for validation. Nonetheless, our test subset results are promising in this regard. Secondly, the inclusion of a wide range of MR imaging examination dates and technical differences may have affected the consistency of results, although this could be considered a positive aspect in terms of generalizability of the method. Thirdly, balancing of cases between tumor types and training and test cohorts was necessary, to solve the biased excess of GB in our sample compared to the general population, however, our test data maintained the specific characteristics of our sample with excess GB, and nonetheless rendered still good results. Lastly, our method involves complex data processing, but we believe it is still

easy to explain as a method intended to improve generalizability by means of nTIC methodology, and to extract the maximum information through the percentile voxel-level analysis.

On the other hand, our study has several strengths. First, the large sample of patients included. Second, the marked technical parameter heterogeneity, which supports credibility and generalizability. Thirdly, the minimal operator dependency with semiautomatic segmentation of enhancing components and automatization of the rest of the process. Fourth, the use of a recently described method of perfusion-curve normalization, favoring reproducibility. Fifth, the application of a completely novel perspective on perfusion-imaging analysis, which considers all time-points and all voxels for the diagnostic model generation, instead of isolated summary parameters. Sixth, the aforementioned comprehensibility which may lead to clinicians' trust in the method and results. And lastly, potential clinical implementation which could be achieved by developing user-friendly tools with visual displays similar to the one presented in figure 4.

Finally, we would like to highlight that we believe the currently proposed method is especially useful in situations in which tissue heterogeneity has important implications, such as this study's, but also in many others, such as radionecrosis versus tumor recurrence, progression versus pseudoprogression, or post-treatment high grade tumors follow-up among others.

CONCLUSION

This proof-of-concept study presents a new perspective on DSC-PWI analysis beyond the interpretation of isolated parameters such as CBV, PSR or PH and their mean or extreme values. Our novel method offers a minimally operator-dependent technique for analyzing every single time-point in the normalized perfusion curves and every single voxel in the tumor and peritumoral area to generate a robust diagnostic model of special interest in heterogeneous tissues and heterogeneous populations.

We also firmly believe that further development and application of this methodology may aid in bridging some of the many problems of comparability and heterogeneity in the field of MR-perfusion imaging. It will facilitate data aggregation and result comparison between studies, promote more robust and generalizable research, and ultimately favor large-scale analyses and clinical implementation.

1. ***Acknowledgements***

   The authors acknowledge support from the Instituto de Salud Carlos III (Proyectos de Investigación en Salud, PI20/00360).

   Funding

   The authors state that this work has not received any funding.

Compliance with Ethical Standards

2. ***Guarantor:***

   The scientific guarantor of this publication is Albert Pons-Escoda.

3. ***Conflict of Interest:***

The authors of this manuscript declare no relationships with any companies, whose products or services may be related to the subject matter of the article.

4. ***Statistics and Biometry:***

   One of the authors has significant statistical expertise: Alonso Garcia-Ruiz (joint first author), Radiomics Group, Vall d'Hebron Institut d'Oncologia.

5. ***Informed Consent:***

   Written informed consent was waived by the Institutional Review Board.

6. ***Ethical Approval:***

   Institutional Review Board approval was obtained.

7. ***Study subjects or cohorts overlap:***

   Some study subjects or cohorts have been previously reported in Pons-Escoda A, Garcia-Ruiz A, Naval-Baudin P, Cos M, Vidal N, Plans G, Bruna J, Perez-Lopez R, Majos C. Presurgical Identification of Primary Central Nervous System Lymphoma with Normalized Time-Intensity Curve: A Pilot Study of a New Method to Analyze DSC-PWI. AJNR Am J Neuroradiol. 2020 Oct;41(10):1816-1824. doi: 10.3174/ajnr.A6761. Epub 2020 Sep 17. PMID: 32943424; PMCID: PMC7661072.

8. ***Methodology***

   - retrospective
   - diagnostic study
   - performed at one institution

REFERENCES

1. Campos S, Davey P, Hird A, et al (2009) Brain Metastasis from an Unknown Primary, or Primary Brain Tumour? A Diagnostic Dilemma. Curr Oncol 16:62–66. https://doi.org/10.3747/co.v16i1.308

2. Ostrom QT, Cioffi G, Gittleman H, et al (2019) CBTRUS Statistical Report: Primary Brain and Other Central Nervous System Tumors Diagnosed in the United States in 2012–2016. Neuro Oncol 21:v1–v100. https://doi.org/10.1093/neuonc/noz150

3. Altwairgi AK, Raja S, Manzoor M, et al (2017) Management and treatment recommendations for World Health Organization Grade III and IV gliomas. Int J Health Sci (Qassim) 11:54–62

4. Enrique G-V, Irving S-R, Ricardo B-I, et al (2019) Diagnosis and management of brain metastases: an updated review from a radiation oncology perspective. J Cancer Metastasis Treat 5:. https://doi.org/10.20517/2394-4722.2019.20

5. Morton LM, Onel K, Curtis RE, et al (2014) The Rising Incidence of Second Cancers: Patterns of Occurrence and Identification of Risk Factors for Children and Adults. Am Soc Clin Oncol Educ B e57–e67. https://doi.org/10.14694/edbook_am.2014.34.e57

6. Donin N, Filson C, Drakaki A, et al (2016) Risk of second primary malignancies among cancer survivors in the United States, 1992 through 2008. Cancer 122:3075–3086. https://doi.org/10.1002/cncr.30164

7. Fuentes-Raspall R, Vilardell L, Perez-Bueno F, et al (2011) Population-based incidence and survival of central nervous system (CNS) malignancies in Girona (Spain) 1994-2005. J Neurooncol 101:117–123. https://doi.org/10.1007/s11060-010-0240-7

8. Patchell RA, Tibbs PA, Walsh JW, et al (1990) A Randomized Trial of Surgery in the Treatment of Single Metastases to the Brain. N Engl J Med 322:494–500. https://doi.org/10.1056/NEJM199002223220802

9. Upadhyay N, Waldman AD (2011) Conventional MRI evaluation of gliomas. Br J Radiol 84:S107–S111. https://doi.org/10.1259/bjr/65711810

10. Fink K, Fink J (2013) Imaging of brain metastases. Surg Neurol Int 4:209. https://doi.org/10.4103/2152-7806.111298

11. Zhang J, Liu H, Tong H, et al (2017) Clinical Applications of Contrast-Enhanced Perfusion MRI Techniques in Gliomas: Recent Advances and Current Challenges. Contrast Media Mol Imaging 1–27. https://doi.org/10.1155/2017/7064120

12. Schmainda K (2016) Perfusion Imaging for Brain Tumor Characterization and Assessment of Treatment Response. In: Handbook of Neuro-Oncology Neuroimaging. Elsevier, pp 335–351

13. Shiroishi MS, Castellazzi G, Boxerman JL, et al (2015) Principles of T 2 *-weighted dynamic susceptibility contrast MRI technique in brain tumor imaging. J Magn Reson Imaging 41:296–313. https://doi.org/10.1002/jmri.24648

14. Welker K, Boxerman J, Kalnin A, et al (2015) ASFNR Recommendations for Clinical Performance of MR Dynamic Susceptibility Contrast Perfusion Imaging of the Brain. Am J Neuroradiol 36:E41–E51. https://doi.org/10.3174/ajnr.A4341

15. Willats L, Calamante F (2013) The 39 steps: evading error and deciphering the secrets for accurate dynamic susceptibility contrast MRI. NMR Biomed 26:913–931. https://doi.org/10.1002/nbm.2833

16. Boxerman JL, Quarles CC, Hu LS, et al (2020) Consensus recommendations for a dynamic susceptibility contrast MRI protocol for use in high-grade gliomas. Neuro Oncol 22:1262–1275. https://doi.org/10.1093/neuonc/noaa141

17. Boxerman JL, Paulson ES, Prah MA, Schmainda KM (2013) The effect of pulse sequence parameters and contrast agent dose on percentage signal recovery in DSC-MRI: Implications for clinical applications. Am J Neuroradiol 34:1364–1369. https://doi.org/10.3174/ajnr.A3477

18. Leu K, Boxerman JL, Ellingson BM (2017) Effects of MRI protocol parameters, preload injection dose, fractionation strategies, and leakage correction algorithms on the fidelity of dynamic-susceptibility contrast MRI estimates of relative cerebral blood volume in gliomas. Am J Neuroradiol. https://doi.org/10.3174/ajnr.A5027

19. Semmineh NB, Bell LC, Stokes AM, et al (2018) Optimization of Acquisition and Analysis Methods for Clinical Dynamic Susceptibility Contrast MRI Using a Population-Based Digital Reference Object. Am J Neuroradiol 39:1981–1988. https://doi.org/10.3174/ajnr.A5827

20. Paulson ES, Schmainda KM (2008) Comparison of Dynamic Susceptibility-weighted Contrast-enhanced MR Methods: Recommendations for Measuring Relative Cerebral Blood Volume in Brain Tumors. Radiology 249:601–613. https://doi.org/10.1148/radiol.2492071659

21. Pekmezci M, Perry A (2013) Neuropathology of brain metastases. Surg Neurol Int 4:245. https://doi.org/10.4103/2152-7806.111302

22. Nduom EK, Yang C, Merrill MJ, et al (2013) Characterization of the blood-brain barrier of metastatic and primary malignant neoplasms. J Neurosurg 119:427–433. https://doi.org/10.3171/2013.3.JNS122226

23. Klekner Á, Hutóczki G, Virga J, et al (2015) Expression pattern of invasion-related molecules in the peritumoral brain. Clin Neurol Neurosurg 139:138–143. https://doi.org/10.1016/j.clineuro.2015.09.017

24. Fidler IJ (2015) The Biology of Brain Metastasis. Cancer J 21:284–293. https://doi.org/10.1097/PPO.0000000000000126

25. Mangla R, Kolar B, Zhu T, et al (2011) Percentage signal recovery derived from MR dynamic susceptibility contrast imaging is useful to differentiate common enhancing malignant lesions of the brain. Am J Neuroradiol 32:1004–1010. https://doi.org/10.3174/ajnr.A2441

26. A Vallée, C Guillevin, M Wager, V Delwail, R Guillevin JV (2018) Added value of spectroscopy to perfusion mrı in the differential diagnostic performance of common malignant brain tumors. AJNR Am J Neuroradiol 39:1423–1431

27. Blasel S, Jurcoane A, Franz K, et al (2010) Elevated peritumoural rCBV values as a mean to differentiate metastases from high-grade gliomas. Acta Neurochir (Wien) 152:1893–1899. https://doi.org/10.1007/s00701-010-0774-7

28. Tsougos I, Svolos P, Kousi E, et al (2012) Differentiation of glioblastoma multiforme from metastatic brain tumor using proton magnetic resonance spectroscopy, diffusion and perfusion metrics at 3 T. Cancer Imaging 12:423–436. https://doi.org/10.1102/1470-7330.2012.0038

29. Neska-Matuszewska M, Bladowska J, Sąsiadek M, Zimny A (2018) Differentiation of glioblastoma multiforme, metastases and primary central nervous system lymphomas using multiparametric perfusion and diffusion MR imaging of a tumor core and a peritumoral zone—Searching for a practical approach. PLoS One 13:e0191341. https://doi.org/10.1371/journal.pone.0191341

30. Cindil E, Sendur HN, Cerit MN, et al (2021) Validation of combined use of DWI and percentage signal recovery-optimized protocol of DSC-MRI in differentiation of high-grade glioma, metastasis, and lymphoma. Neuroradiology 63:331–342. https://doi.org/10.1007/s00234-020-02522-9

31. Cha S, Lupo JM, Chen MH, et al (2007) Differentiation of glioblastoma multiforme and single brain metastasis by peak height and percentage of signal intensity recovery derived from dynamic susceptibility-weighted contrast-enhanced perfusion MR imaging. Am J Neuroradiol 28:1078–1084. https://doi.org/10.3174/ajnr.A0484

32. Law M, Cha S, Knopp EA, et al (2002) High-grade gliomas and solitary metastases: Differentiation by using perfusion and proton spectroscopic MR imaging. Radiology 222:715–721. https://doi.org/10.1148/radiol.2223010558

33. Rollin N, Guyotat J, Streichenberger N, et al Clinical relevance of diffusion and

perfusion magnetic resonance imaging in assessing intra-axial brain tumors. Springer

34. Wang S, Kim S, Chawla S, et al (2011) Differentiation between Glioblastomas, Solitary Brain Metastases, and Primary Cerebral Lymphomas Using Diffusion Tensor and Dynamic Susceptibility Contrast-Enhanced MR Imaging. Am J Neuroradiol 32:507–514. https://doi.org/10.3174/ajnr.A2333

35. Server A, Orheim TED, Graff BA, et al (2011) Diagnostic examination performance by using microvascular leakage, cerebral blood volume, and blood flow derived from 3-T dynamic susceptibility-weighted contrast-enhanced perfusion MR imaging in the differentiation of glioblastoma multiforme and brain me. Neuroradiology 53:319–330. https://doi.org/10.1007/s00234-010-0740-3

36. Chiang IC, Kuo YT, Lu CY, et al (2004) Distinction between high-grade gliomas and solitary metastases using peritumoral 3-T magnetic resonance spectroscopy, diffusion, and perfusion imagings. Neuroradiology 46:619–627. https://doi.org/10.1007/s00234-004-1246-7

37. Askaner K, Rydelius A, Engelholm S, et al (2019) Differentiation between glioblastomas and brain metastases and regarding their primary site of malignancy using dynamic susceptibility contrast MRI at 3T. J Neuroradiol 46:367–372. https://doi.org/10.1016/j.neurad.2018.09.006

38. Lee MD, Baird GL, Bell LC, et al (2019) Utility of Percentage Signal Recovery and Baseline Signal in DSC-MRI Optimized for Relative CBV Measurement for Differentiating Glioblastoma, Lymphoma, Metastasis, and Meningioma. Am J Neuroradiol 40:1145–1450. https://doi.org/10.3174/ajnr.A6153

39. Hakyemez B, Erdogan C, Bolca N, et al (2006) Evaluation of different cerebral mass lesions by perfusion-weighted MR imaging. J. Magn. Reson. Imaging 24:817–824

40. Calli C, Kitis O, Yunten N, et al (2006) Perfusion and diffusion MR imaging in enhancing malignant cerebral tumors. Eur J Radiol 58:394–403. https://doi.org/10.1016/j.ejrad.2005.12.032

41. Bulakbasi N, Kocaoglu M, Farzaliyev A, et al (2005) Assessment of diagnostic accuracy of perfusion MR imaging in primary and metastatic solitary malignant brain tumors. Am J Neuroradiol 26:2187–2189

42. Pons-Escoda A, Garcia-Ruiz A, Naval-Baudin P, et al (2020) Presurgical Identification of Primary Central Nervous System Lymphoma with Normalized Time-Intensity Curve: A Pilot Study of a New Method to Analyze DSC-PWI. Am J Neuroradiol 41:1816–1824. https://doi.org/10.3174/ajnr.A6761

43. Louis DN, Ohgaki H, Wiestler OD, et al (2007) The 2007 WHO Classification of Tumours of the Central Nervous System. Acta Neuropathol 114:97–109. https://doi.org/10.1007/s00401-007-0243-4

44. Wen PY, Huse JT (2017) 2016 World Health Organization Classification of Central Nervous System Tumors. Contin Lifelong Learn Neurol 23:1531–1547. https://doi.org/10.1212/CON.0000000000000536

45. Hochberg FH, Pruitt A (1980) Assumptions in the radiotherapy of glioblastoma. Neurology 30:907–907. https://doi.org/10.1212/WNL.30.9.907

46. Wallner KE, Galicich JH, Krol G, et al (1989) Patterns of failure following treatment for glioblastoma multiforme and anaplastic astrocytoma. Int J Radiat Oncol 16:1405–1409. https://doi.org/10.1016/0360-3016(89)90941-3

47. Gaspar LE, Fisher BJ, Macdonald DR, et al (1992) Supratentorial malignant glioma: Patterns of recurrence and implications for external beam local treatment. Int J Radiat Oncol 24:55–57. https://doi.org/10.1016/0360-3016(92)91021-E

48. Liang BC, Thornton AF, Sandler HM, Greenberg HS (1991) Malignant astrocytomas: focal tumor recurrence after focal external beam radiation therapy. J Neurosurg 75:559–563. https://doi.org/10.3171/jns.1991.75.4.0559

49. Mandrekar JN (2010) Receiver Operating Characteristic Curve in Diagnostic Test Assessment. J Thorac Oncol 5:1315–1316. https://doi.org/10.1097/JTO.0b013e3181ec173d

50. Tate AR, Underwood J, Acosta DM, et al (2006) Development of a decision support system for diagnosis and grading of brain tumours usingin vivo magnetic resonance single voxel spectra. NMR Biomed 19:411–434. https://doi.org/10.1002/nbm.1016

TABLES

Table1. Demographics of study participants.

Table2. Summary of the results.

Supplemental Table1. Imaging acquisition parameters ranges for DSC-PWI and T1CE-wi.

Supplemental Table2. Summary of DSC-PWI pulse-sequence parameters and their distribution into the study subgroups.

FIGURES

Figure1. Study participants flow-chart.

Figure2. Overlapped average nTICs of glioblastoma (line) and metastasis (dashed line), discriminatory time-points highlighted by an X, and generated algorithms; everything obtained in the training set. Upper-row for enhancing tumor, lower-row for peritumoral region. The algorithms depict the best percentile (p) for each time point (X) and the relative power for each combination.

Figure3. Graphic representation of AUC-ROC in training (left) and test (right) groups, for enhancing tumor (line), peritumoral region (dashed line) and matching combinations (lower row). Training (enhancing tumor AUC = 0.81, peritumoral region AUC = 0.83, matching combined AUC = 0.90). Test (enhancing tumor AUC = 0.79, peritumoral region AUC = 0.71, matching combined AUC = 0.84). All significant ($p<0.00015$).

Figure4. Example problem case. Axial T1CE-wi shows an intraaxial, frontal and insular, enhancing, necrotic tumor which could correspond to a GB or to a single brain metastasis. The results of the algorithms applied to the problem case (represented by an X) are overlapped to scattered boxplots of our training set, those facilitating a visual assessment of the diagnostic classification probability. In this problem case, the classification favors single brain metastasis for both the enhancing tumor and peritumoral region. Pathology confirmed this tumor corresponded to a renal cell carcinoma single brain metastasis.

Tables

Table1. Demographics.

Tumor types

	Cases	Men	Women	Age
Glioblastoma	321	197	124	60 (20-86)
Metastasis	107	59	48	60 (24-81)
Total	428	256	172	60 (20-86)

Study subgroups

	Cases	Men	Women	Age
Train	146	93	53	59 (26-86)
Test	276	178	98	60 (20-86)
Total	422	253	169	60 (20-86)

Table2. Summary of the results in training and test subsets.

	AUC	Accuracy	Sensitivity	Specificity
Enhancing Tumor				
Training	**0.81**	78% (114/146)	71% (52/73)	85% (62/73)
Test	**0.79**	71% (195/276)	84% (26/31)	69% (169/245)
Peritumoral Region				
Training	**0.83**	78% (114/146)	70% (51/73)	86% (63/73)
Test	**0.71**	65% (179/276)	55% (17/31)	66% (162/245)
Combined	**Match**	**Accuracy**	**Sensitivity**	**Specificity**
Training	72% (105/146)	**88% (92/105)**	86% (44/51)	89% (48/54)
Test	61% (169/276)	**81% (135/169)**	75% (13/16)	80% (122/153)

Figure 1

Click here to access/download;Figure;FIG1.jpg

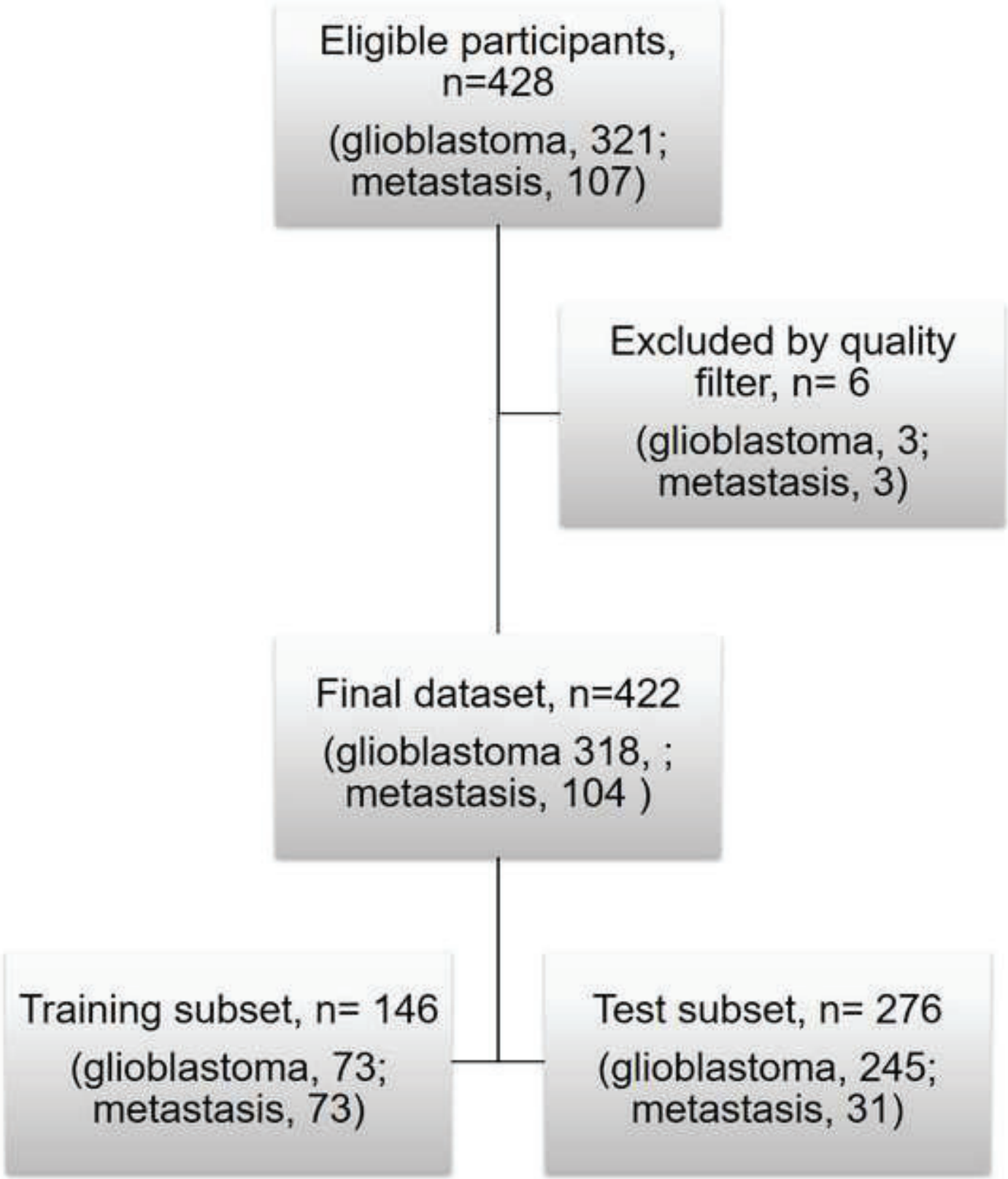

Figure 2

Click here to access/download;Figure;FIG2.jpg

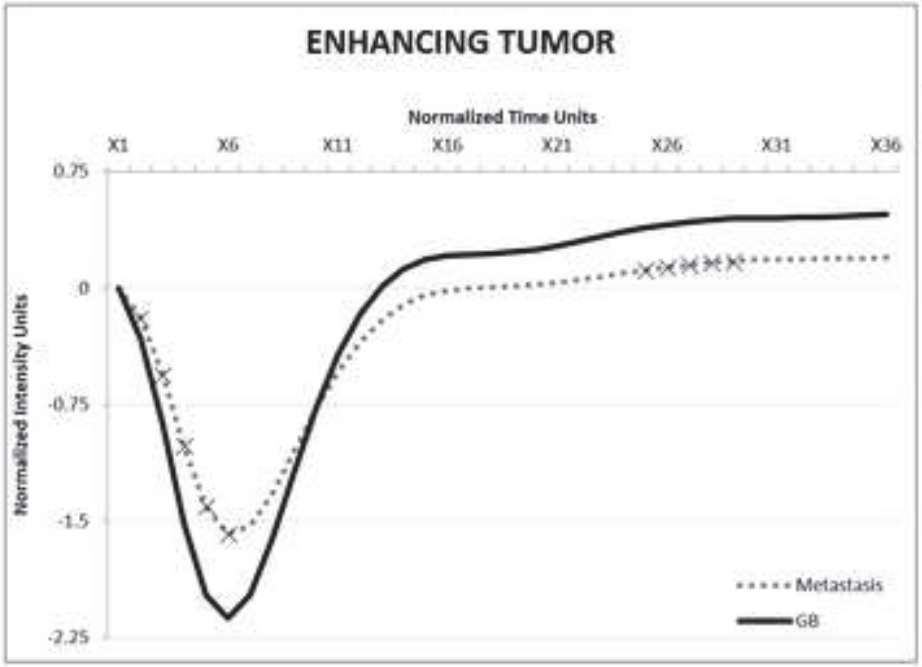

Enhancing Tumor	
variables	coefficients
(Intercept)	1.6399319
p60 $X2_i$	5.3447739
p70 $X3_i$	-0.380345
p75 $X4_i$	4.4540826
p85 $X5_i$	-4.3117039
p95 $X6_i$	3.9044655
p95 $X25_i$	0.7014149
p60 $X26_i$	-1.4883295
p60 $X27_i$	-22.8331364
p60 $X28_i$	20.3161906
p60 $X29_i$	1.6134529

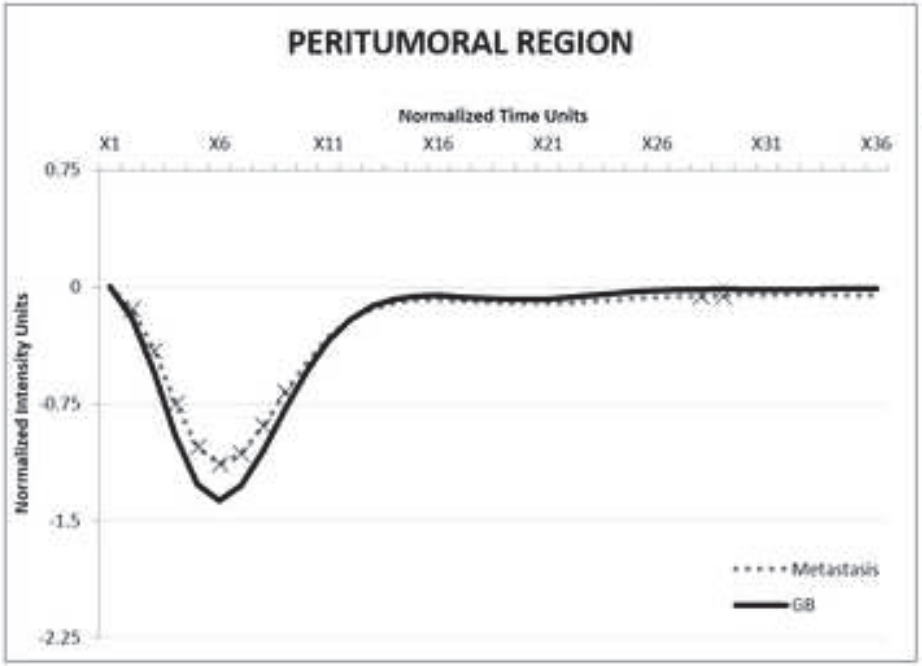

Peritumoral Region	
variables	coefficients
(Intercept)	2.936152
p70 $X2_i$	-48.899096
p65 $X3_i$	63.173447
p85 $X4_i$	-3.468098
p90 $X5_i$	10.997735
p90 $X6_i$	-8.478254
p95 $X7_i$	1.766047
p90 $X8_i$	25.776699
p75 $X9_i$	-13.559063
p20 $X28_i$	5.333112
p20 $X29_i$	-10.130743

Figure 3

Click here to access/download;Figure;FIG3.jpg

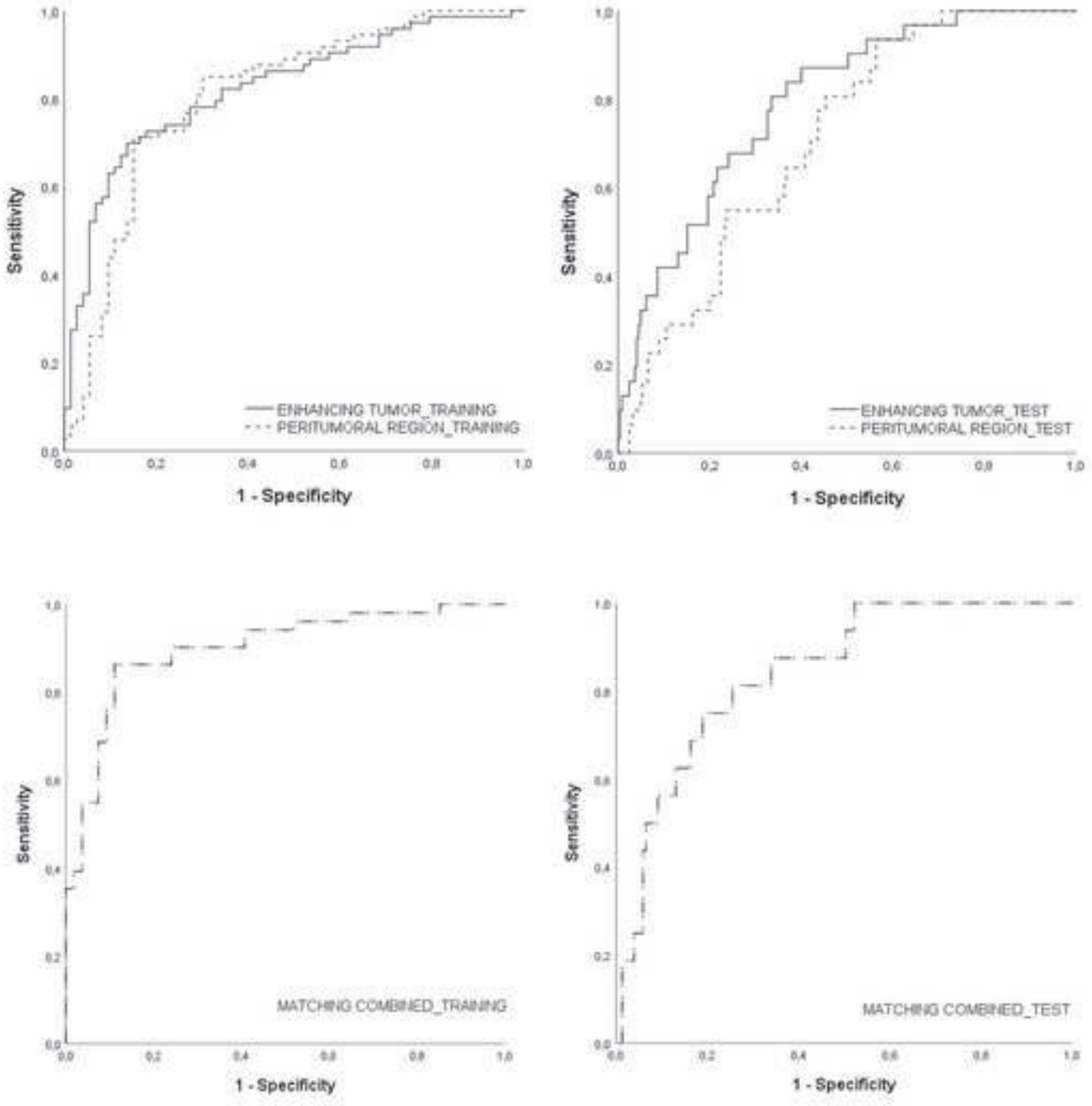

Figure 4

Click here to access/download;Figure;FIG4.jpg

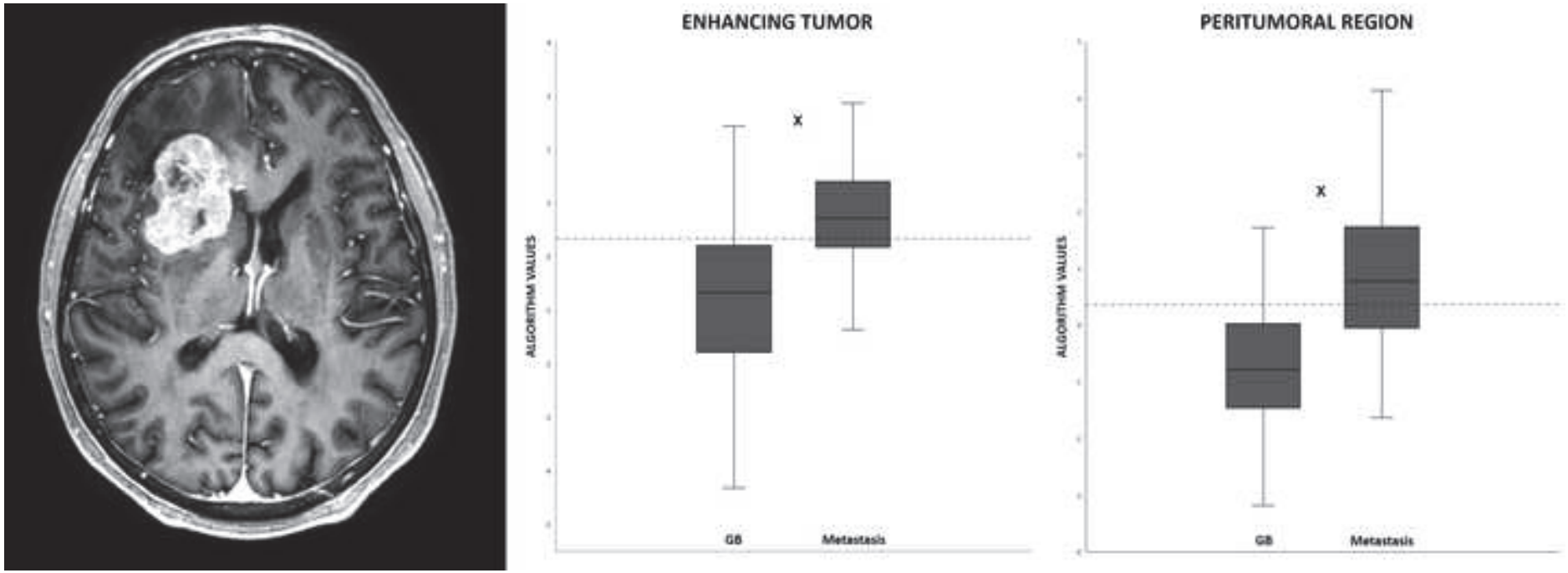

1. ***Acknowledgements***

The authors acknowledge support from the Instituto de Salud Carlos III (Proyectos de Investigación en Salud, PI20/00360).

Funding

The authors state that this work has not received any funding.

Compliance with Ethical Standards

2. ***Guarantor:***

The scientific guarantor of this publication is Albert Pons-Escoda.

3. ***Conflict of Interest:***

The authors of this manuscript declare no relationships with any companies, whose products or services may be related to the subject matter of the article.

4. ***Statistics and Biometry:***

One of the authors has significant statistical expertise: Alonso Garcia-Ruiz (joint first author), Radiomics Group, Vall d'Hebron Institut d'Oncologia.

5. ***Informed Consent:***

Written informed consent was waived by the Institutional Review Board.

6. ***Ethical Approval:***

Institutional Review Board approval was obtained.

7. ***Study subjects or cohorts overlap:***

Some study subjects or cohorts have been previously reported in Pons-Escoda A, Garcia-Ruiz A, Naval-Baudin P, Cos M, Vidal N, Plans G, Bruna J, Perez-Lopez R, Majos C. Presurgical Identification of Primary Central Nervous System Lymphoma with Normalized Time-Intensity Curve: A Pilot Study of a New Method to Analyze DSC-PWI. AJNR Am J Neuroradiol. 2020 Oct;41(10):1816-1824. doi: 10.3174/ajnr.A6761. Epub 2020 Sep 17. PMID: 32943424; PMCID: PMC7661072.

8. ***Methodology***

- retrospective
- diagnostic study
- performed at one institution